Chemical Engineering Journal 109 (2005) 1–9

Chemical Engineering Journal

www.elsevier.com/locate/cej

Lumps and kinetics for the secondary reactions in catalytically cracked gasoline

Longyan Wang, Bolun Yang *, Zhiwen Wang

Department of Chemical Engineering, Xi'an Jiaotong University, Xi'an 710049, PR China

Received 29 September 2004; received in revised form 25 February 2005; accepted 28 February 2005

Abstract

The secondary reactions of catalytically cracked gasoline have been investigated with a riser reactor using an improved Y zeolite catalyst in different operating conditions. All the reactions that will take place in this system, such as cracking reactions, hydrogen transfer reactions, aromatization reactions, isomeration reactions, alkylation reactions, and dimerization reactions, etc. were analyzed. This reaction system was cut into dry gas lump (DG), liquefied petroleum gas lump (LPG), light cycle oil lump (LCO), coke lump (COKE), and gasoline lump (GL) in accordance with the product structure of commercial fluid catalytic cracking unit (FCCU); the lump GL could be cut into paraffin lump (GP), olefin lump (GO), naphthene lump (GN), and aromatic lump (GA) further according to the hydrocarbon group structure. The eight-lump kinetic model for this reaction system thus could be developed and the hybrid genetic algorithm was used to obtain the model parameters. The kinetic parameters calculated from the improved genetic algorithm are reliable, and the calculated data of the product distribution were agreed well with the experimental results. The model offers the function of predicting the levels of olefins, aromatics, etc. in gasoline products after secondary reactions.

Keywords: Fluid catalytic cracking; Gasoline; Secondary reaction; Lumping; Kinetics; Hybrid genetic algorithm

1. Introduction

It is well known that catalytic cracking of heavy hydrocarbons on zeolite catalysts is complex parallel–series reaction in carbonium ion mechanism. Direct cracking, dehydrogenation, and condensation reactions of the feedstock, which produce gasoline, diesel, liquefied petroleum gas (LPG), coke, and dry gas, are regarded as primary reactions. As middle products, gasoline and diesel produced in primary reactions will conduct secondary reactions including cracking, hydrogen transfer, isomeration, aromatization, alkylation, condensation, etc. John and Wojciechowski have investigated catalytic cracking of gas oil and set up a reaction network of primary reactions and secondary reactions [1]. By the relationship between conversion and yields of products, they concluded that primary reactions of gas oil only produce gasoline, butylenes, *n*-butylenes, and propylene, and that all other products such as ethylene, coke, etc. are formed by secondary reactions. Also, secondary reactions of gasoline bring butylenes, *n*-butylenes, and propylene.

Over the past decades, restricting secondary reactions have always been one of the key goals for developing new fluid catalytic cracking (FCC) technologies including catalyst, reactor, and process optimization to maximize the resid oil ratio in feed, gasoline yield, and octane number, and to minimize coke and dry gas yields. Many lumping kinetic models have been developed for the process optimization. These models can be categorized into two types. One is that the lumps are gained based on the boiling range of feed stocks and corresponding products in the reaction system, such as the three-lump model by Weekman and Nace [2,3], the five-lump models by Corella and Frances [4] and by Ancheyta-Juarez et al. [5], and the seven-lump model by Sugungun et al. [6]. This kind of model has an increasing trend in the lump number of the cracked gas components. The other is that the lumps are gained on the basis of molecular structure characteristics of hydrocarbon group composition in reaction system, such

* Corresponding author. Tel.: +86 29 82668980; fax: +86 29 83237910.
E-mail address: blunyang@mail.xjtu.edu.cn (B. Yang).

1385-8947/$ – see front matter © 2005 Elsevier B.V. All rights reserved.
doi:10.1016/j.cej.2005.02.024

Nomenclature

a_j	concentration of jth lump in vapor ($\text{mol}_j\ \text{g}_{\text{vapor}}^{-1}$)
$\vec{a}$	vector of concentration of lumps
E	activation energy (J mol^{-1})
G_V	vapor mass flow rate cross the riser ($\text{g m}^{-2}\ \text{s}^{-1}$)
k_j	reaction rate constant of lump j ($\text{m}^3\ (\text{g}_{\text{cat}}\ \text{s})^{-1}$)
$\vec{K}$	rate constants matrix
L	effective length of riser reactor (m)
m	times of experiments
M_j	molecular weight of lump j (g mol^{-1})
$\overline{\text{MW}}$	average molecular weight of vapor mixture (g mol^{-1})
n	lumps number
P	reaction pressure (Pa)
r_j	reactive rate of lump j ($\text{mol m}^{-3}\ \text{s}^{-1}$)
R	gas constant ($R = 8.3143\ \text{J (mol K)}^{-1}$)
t	time from reaction beginning (s)
t_v	vapor residence time ((s) $t_v = L/u$)
T	reaction temperature (K)
u	vapor flow velocity in bed (m s^{-1})
x	distance from reactor entrance (m)
X	relative distance with no dimension ($X = x/L$)
y_j	yield of lump j
y_j^c	calculated yield
y_j^e	experimental yield

Greek letters

γ	stoichiometric coefficient
ε	void volume fraction of fluidized bed
ρ	vapor density (g m^{-3})
ρ_c	catalyst bed density (g m^{-3})
$\varphi_{c/o}$	catalyst to oil ratio

as the 10-lump model by Gross et al. [7], and the 13-lump model by Deng et al. [8]. These models emphasize the description in more details for the feedstock. Both the available lumping kinetic models, however, neglect the composition of gasoline—the most important FCC product and fail to take the peculiarity of olefin molecules in the system into account. It is evident that the application of these models would be affected currently due to the worldwide request for FCC units to produce the clean fuel gasoline component with low olefins and low aromatics.

The olefin issue in FCC process is paid more and more attention nowadays, because not only FCC units are urged to yield low olefin gasoline blending components, but also refiners pursue increasing propylene and *iso*-butylene yields for higher profit margin. Some catalyst companies and refining technology licensors have successfully developed several technologies to produce low olefin gasoline and/or to raise propylene yields from FCC units by use of the secondary reactions of FCC gasoline. New catalysts for reducing FCC gasoline olefins reported by Raymond et al. [9] and Ye et al. [10] can selectively promote certain secondary reactions like olefins cracking and hydrogen transfer by introducing special active substance into catalysts. Xu et al. [11] and Wang et al. [12] reported separately new FCC processes reducing gasoline olefin or increasing propylene yields, in which reactors have been improved to provide FCC naphtha secondary reactions with adequate reaction time, space, and advantageous condition. Designing and operating optimally the new processes require investigating the kinetics of FCC gasoline secondary reactions, including reactive behavior of gasoline olefins. It is necessary to establish a kinetic model for gasoline secondary reactions that is capable of predicting gasoline paraffin, olefin, naphthene, and aromatic (PONA) composition.

FCC naphtha secondary reactions involve hundreds of hydrocarbon molecules and thousands of chemical reactions, among which there are complicated mutual influences. It is far from enough to explain the whole reaction mechanism by investigating several typical reactions lonely. At the same time, it is difficult to solve the gasoline secondary reaction network with conventional methods of solving kinetic models for complicated reaction system. In this work, the secondary reactions system was divided into eight lumps based on the experimental results. Each lump is regarded as a pseudo-molecule and its kinetic behavior is researched in light of the lumping theory found by Wei and Kue [13,14]. The eight-lump kinetic model was set up on the basis of the characteristics of secondary reactions of catalytically cracked gasoline and the experimental results. The hybrid genetic algorithm [20] was used to obtain the model parameters, which in turn were verified with the experimental data.

2. Kinetic model

2.1. Analysis for the secondary reactions of FCC gasoline

FCC gasoline fraction consists mainly of paraffins (P), olefins (O), naphthenes (N), and aromatics (A) with C_5–C_{11}, and a small quantity of non-hydrocarbon compounds containing oxygen, sulfur, or nitrogen. Generally, the PONA composition of gasoline can be analyzed by fluorescence indicator method or gas chromatograph method. Olefin, accounting for 35–60 vol.% of typical FCC gasoline, is the most unstable lump among four hydrocarbon groups in catalytically cracked gasoline. The secondary reactions of FCC gasoline mostly refer to the chemical reactions containing olefin participants. When the reaction temperature is in 773–923 K and with catalysis of Y or ZSM-5 zeolite catalysts. Secondary reactions of FCC gasoline are shown as follows [12,15]:

(1) cracking reactions:
- cracking reactions of olefin molecules, e.g., $C_7H_{14}\,(O) \rightarrow C_4H_8 + C_3H_6$

- cracking reactions of paraffin molecules, e.g.,

  $C_6H_{14} \rightarrow C_3H_8 + C_3H_6$

  (in carbonium ion mechanism)

  $C_7H_{14} \rightarrow C_5H_{10} + C_2H_4$ (in free radical mechanism)
- ring breaking reactions of naphthene molecules, e.g., C_6H_{12} (N) $\rightarrow$ C_6H_{12} (O) $\rightarrow$ C_3H_6
- substituent breaking reactions of aromatic molecules, e.g., $C_3H_7{\cdot}C_6H_5$ (A) $\rightarrow$ C_6H_6 (A) + C_3H_6;

(2) hydrogen transfer reactions, representing many dual-molecule reactions related with olefins and producing hydrogen-sufficient saturates and hydrogen-deficient aromatics, including:
- reactions between olefin molecules, e.g., 4 C_6H_{12} (O) $\rightarrow$ 3 C_6H_{14} + C_6H_6 (A)
- reactions between olefin and naphthene molecules, e.g., C_6H_{12} (N) + 3 i-C_5H_{10} $\rightarrow$ 3 C_5H_{12} + C_6H_6 (A)
- reactions between olefin and coke precursor molecules, e.g., coke precursor + C_nH_{2n} $\rightarrow$ coke + C_nH_{2n+2};

(3) aromatization reactions, i.e., aromatic-forming reactions from paraffins, olefins, and naphthenes, including:
- reactions of naphthenes dehydrogenating directly to form aromatics, e.g., C_6H_{12} (N) $\rightarrow$ C_6H_6 (A) + 3 H_2
- reactions of olefins dehydrocyclization, e.g., C_7H_{14} (O) $\rightarrow$ C_7H_{14} (N) $\rightarrow$ C_7H_8 (A) + 3 H_2;

(4) isomeration reactions, including:
- framework isomeration reactions of paraffins, olefins, and naphthenes, e.g., n-$C_5H_{12} \rightarrow$ $CH_3{\cdot}C_4H_9$; l-$C_4H_8 \rightarrow$ i-C_4H_8; C_6H_{12} (N) $\rightarrow$ $CH_3{\cdot}C_5H_9$ (N)
- double bond isomeration reactions of olefins, e.g., l-$C_4H_8 \rightarrow$ t-2-C_4H_8
- isomeration reactions of aromatics, e.g., o-$C_6H_4(CH_3)_2 \rightarrow$ m-$C_6H_4(CH_3)_2$;

(5) alkylation and dimerization reactions, e.g.,

$2\,n\text{-}C_6H_{12} \rightarrow n\text{-}C_{12}H_{24}$

C_6H_6 (A) + $C_2H_4 \rightarrow$ $C_2H_5{\cdot}C_6H_5$ (A);

(6) condensation, dehydrogenation, and coke-make reactions, e.g.,

$CH_2{=}CH{-}C_6H_5 + R_1CH{=}CHR_2 \rightarrow$ cokeprecursor + H_2

cokeprecursor + $C_nH_{2n} \rightarrow$ coke + C_nH_{2n+2}

$C_7H_{16} \rightarrow C_7H_{14}$ (O) + H_2.

2.2. Physical model

The secondary reactions of FCC naphtha in different operating conditions have been tested with a riser reactor catalytic cracking experimental unit. The results indicate that secondary reactions make a great change in the PONA composition of naphtha itself. The reactions produce lighter cracked products LPG and dry gas, and heavier condensed products coke and diesel fraction similar to FCC light cycle oil (LCO) in property. Based on above results, the material system of secondary reactions can be plotted five lumps in accordance with feedstock and product structure. These lumps include dry gas lump (DG, H_2 and C_1–C_2), liquefied petroleum gas lump (LPG, C_3–C_4), gasoline lump (GL, $C_5{}^+$–477 K), light cycle oil lump (LCO, >477 K), and coke lump (COKE). Since the lump GL represents both feedstock and product, the PONA compositions will be changed during the reaction process, it is reasonable to divide the lump GL according to the hydrocarbon group structure into paraffin lump (GP), olefin lump (GO), naphthene lump (GN), and aromatic lump (GA). Thus, the reaction system is cut into eight lumps totally.

It can be known from Section 2.1 that secondary reactions of FCC naphtha are rather complicated. Realizing that different groups of hydrocarbons have different reactive behaviors, to simplify the reaction scheme, following assumptions can be considered:

(1) All the reactions are regarded as first-order reactions.
(2) Lumps GP, GO, and GN can be converted each other; these reactions are considered as reversible reactions among the lumps in the model.
(3) LPG only converted to dry gas, LCO only converted to coke, and there is no interaction between dry gas and coke.
(4) There are few $C_3{}^+$ alkyl aromatics in FCC naphtha; the model considers aromatics not forming LPG directly and lump GP not producing LCO directly, either.
(5) Lump GA does not yield lump GN directly for the reason of reacting in nearly atmospheric pressure.
(6) Influence of sulfur and nitrogen in compounds on secondary reactions is neglected.

Following the reaction mechanism and above assumptions, a kinetic physical model of secondary reactions of catalytically cracked gasoline was proposed, shown in Fig. 1.

There are 21 reactions in the system of secondary reactions network; obviously, 21 reaction rate constants are needed.

2.3. Activation energy and catalyst decay

In this work, Arrhenius empiric formula ($k = k_0 \exp(-E/RT)$) is used to calculate the activation energy data of reactions by means of the reaction rate constants determined in different temperatures.

In conventional FCC process, Y or ZSM-5 zeolite catalysts deactivate rapidly because of coke formation on catalyst. Most previous kinetic models for catalytic cracking took

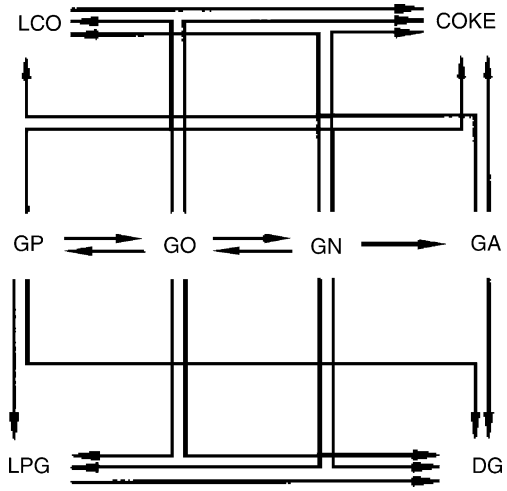

Fig. 1. Reactive scheme of the eight-lump kinetic model for FCC gasoline secondary reactions.

catalyst activity as function of coke content on catalysts or time-on-stream of catalyst. Since the coke on catalyst for gasoline feed is normally less than 0.20 wt% even when the reaction finishes, the catalyst decay thus is neglected in this work.

2.4. Stoichiometric coefficient and molecular weight

Each reaction between lumps in the kinetic models has its own stoichiometric coefficient. For example, reaction $J \rightarrow \gamma I$, the stoichiometric coefficient will be $\gamma_{ji} = M_j/M_i$. The average molecular weight of each lump except coke may be accurately calculated by means of analyzing its components. Coke is a highly condensed polymer of hydrocarbons, a solid absorbed on catalyst surface. Coke yield can be achieved with other lumps' yields; therefore, the molecular weight and stoichiometric coefficients of the coke may not be taken into account. By component analysis data of feed and products of FCC gasoline secondary reaction, the average molecular weight of every lump and corresponding stoichiometric coefficient between different lumps have been calculated as shown in Table 1.

2.5. Continuity equation

Since FCC gasoline secondary reaction time in riser reactors is very short (less than 5 s), the reversible reactions within lump GL are far from away chemical equilibrium in normal operating conditions. It is reasonable to treat these reversible reactions as first-order irreversible reactions. The following assumptions are made on developing the mathematical model for the riser reactor:

(a) Reactor hydrodynamics are isothermal plug flow and ideally mixed.
(b) Reactions progress is limited only by chemical reaction, and internal and external diffusions are neglected.
(c) Reactants are uniformly absorbed on a surface of catalyst with ideally distributed active sites.

A continuity equation in riser reactor can be written as:

$$\left(\frac{\partial \rho a_j}{\partial t}\right)_x + G_V\left(\frac{\partial a_j}{\partial x}\right)_t = r_j \tag{1}$$

If cross-section area of the riser and mass velocity of the material stream are invariant, then

$$G_V = \rho u = \text{constant} \tag{2}$$

The disappearance rate of lump j is in direct proportion to its mole concentration ρa_j and the mass density of catalyst to gas volume (ρ_c/ε):

$$r_j = -k_j \rho a_j \left(\frac{\rho_c}{\varepsilon}\right) \tag{3}$$

From Eqs. (1) and (3), Eq. (4) can be derived:

$$\left(\frac{\partial \rho a_j}{\partial t}\right)_x + G_V\left(\frac{\partial a_j}{\partial x}\right)_t = -k_j \rho a_j \left(\frac{\rho_c}{\varepsilon}\right) \tag{4}$$

When the reaction process in riser reactors keeps in stability, the partial derivative item in the left of Eq. (4) equals to zero. By the definition of G_V:

$$G_V = \frac{(\rho_c/\varepsilon)L}{\varphi_{c/o} t_v} = \frac{(\rho_c/\varepsilon)L}{\varphi_{c/o}(L/u)} \tag{5}$$

Treating the stream vapor in reactor as ideal gas, then:

$$\rho = \frac{P\overline{\mathrm{MW}}}{RT} \tag{6}$$

Replacing the actual distance by the relative distance with no dimension, Eq. (4) can be re-written as:

$$\frac{\mathrm{d}a_j}{\mathrm{d}X} = -\frac{P\overline{\mathrm{MW}}}{RT}\varphi_{c/o} t_v k_j a_j \tag{7}$$

Expressed in matrix:

$$\frac{\mathrm{d}\vec{a}}{\mathrm{d}X} = \frac{P\overline{\mathrm{MW}}}{RT}\varphi_{c/o} t_v \vec{K}\vec{a} \tag{8}$$

Turning the concentration a_j into the yield y_j:

$$y_j = a_j M_j; \quad j = 1, 7 \tag{9}$$

The yield of coke, which is a solid deposit on the surface of the deactivation catalyst, could be calculated through a mass

Table 1
Average molecular weights and stoichiometric coefficients

Lumps	GP	GO	GN	GA	LCO	LPG	DG
M_j (g mol^{-1})	102	100	100	90	187	48	21
GP	–	1.02	–	–	–	2.13	4.86
GO	0.98	–	1.0	–	0.53	2.08	4.76
GN	–	1.0	–	1.11	0.53	2.08	4.76
GA	–	–	–	–	0.48	–	4.29
LPG	–	–	–	–	–	–	2.29

balance:

$$y_{\mathrm{COKE}} = 1 - \sum_{j=1}^{7} a_j M_j \tag{10}$$

The average molecular weight of vapor mixture ($\overline{\mathrm{MW}}$) can be expressed by:

$$\overline{\mathrm{MW}} = \frac{\sum_{j=1}^{7} a_j M_j}{\sum_{j=1}^{7} a_j} = \frac{1}{\sum_{j=1}^{7} a_j} \tag{11}$$

For the riser reactor, eight-lump kinetic model can be expressed by:

$$\left\{ \begin{array}{c} \dfrac{\mathrm{d}\vec{a}}{\mathrm{d}X} = \dfrac{p\varphi_{\mathrm{c/o}}}{RT\sum_{j=1}^{7} a_j} \left(\dfrac{L}{u}\right) \vec{K}\vec{a} \\ y_j = a_j M_j;\ j = 1, 7 \\ y_{\mathrm{COKE}} = 1 - \sum_{j=1}^{7} a_j M_j \end{array} \right\} \tag{12}$$

where $\vec{K}$ represents rate constants matrix; $\vec{a} = [a_1, a_2, \cdots, a_7]^{\mathrm{T}}$, a_1, a_2, …, a_7 represent the concentrations of lumps GP, GO, GN, GA, LCO, LPG, and DG, respectively.

Eq. (12) is the basic equations for the eight-lump kinetic model of FCC gasoline secondary reactions, in which the key operating parameters for secondary reactions of catalytically cracked gasoline such as temperature (T), pressure (P), residence time (t_{v}) of oil vapor, and catalyst to oil ratio ($\varphi_{\mathrm{c/o}}$) are involved.

3. Experimental

3.1. Experimental unit

All the experimental runs on FCC naphtha secondary reactions were performed in a continuous catalytic cracking unit with a riser reactor, shown in Fig. 2. The unit contained 5 kg catalyst in total, continuously circulating operation of reaction–regeneration could be carried out with a feed rate of 0.5–2.0 kg/h. The riser reactor, 2800 mm in length, was made of stainless steel pipe Ø 22 × 3 mm. Pressure balance and catalyst circulating rate were adjusted by means of four special valves installed separately in the flue pipe, reactive effluent pipe, spent catalyst pipe, and regenerated catalyst pipe. Control for the key operating parameters and the data collection were carried out by a computer. The whole unit was electrically heated and the catalyst-circulating rate was independent on the heat balance.

3.2. Analysis of feeds and products

Gaseous products were analyzed by a multi-dimension gas chromatography, model HP 6890, with four valves, two thermal conductivity detectors (TCDs), and five packed columns. Liquid products were cut into gasoline fractions (C_5^+−477 K) and LCO fractions (>477 K) in a laboratory unit of real boiling point distillation. PONA compositions of feed and product gasoline fractions were achieved by gas chromatographic procedure described by ASTM D-6733-2001. The coke yield was calculated using flue gas volume and CO_2 content analyzed by an infrared analyzer.

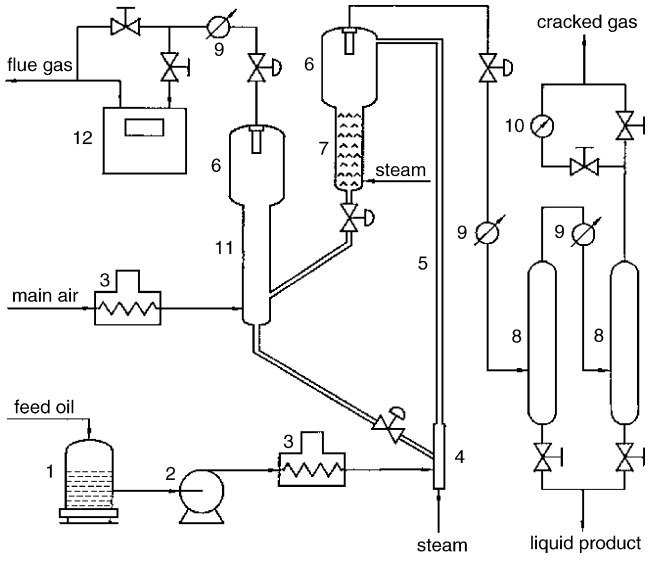

Fig. 2. Schematic diagram of continuous catalytic cracking experimental unit with riser reactor; (1) feed tank; (2) feed pump; (3) preheater; (4) injection nozzle; (5) riser reactor; (6) gas–solid separator; (7) stripper; (8) liquid product receiver; (9) cooler; (10) cracked gas meter; (11) regenerator; (12) flue gas meter.

3.3. Feeds and catalyst

The feeds, three samples of catalytically cracked naphtha, used in this work were taken from the industrial FCC units of China. Their properties are shown in Table 2. Catalyst used in the experiments, CC-20D (manufactured by Sinopec Changling Catalyst Co. Ltd., China), is an equilibrium catalyst taken from the circulating inventory of a commercial FCC unit. Its properties are shown in Table 3.

Table 2
Properties of the feedstock used in the experiments

Feed samples code	Feed no. 1	Feed no. 2	Feed no. 3
Boiling range (K)	305–451	310–459	312–439
Density at 293 K (kg m^{-3})	708.4	732.4	705.8
Sulfur (ppm)	380	1427	288
Octane number (RON)	90.6	91.3	90.5
Paraffins (vol.%)	34.3	30.7	36.1
Olefins (vol.%)	44.5	41.8	35.2
Naphthenes (vol.%)	7.4	9.4	13.7
Aromatics (vol.%)	13.8	18.1	15.0

Table 3
Properties of the catalyst CC-20D (E-Cat) used in the experiments

Item	Value
Surface area ($m^2\ g^{-1}$)	98.0
Pore volume ($ml\ g^{-1}$)	0.14
Apparent bulk density ($g\ ml^{-1}$)	0.84
Carbon on Reg. Cat (wt%)	0.08
Micro activity, MA	59.9
Al_2O_3 (wt%)	45.2
Nickel (ppm)	9800
Vanadium (ppm)	940
Sodium (ppm)	2290

4. Results and discussion

4.1. Secondary reaction results

All the experimental runs of three naphtha feedstock are carried out under a pressure of 0.113 MPa. As the main operating variables affected the depth of the secondary reactions, the effects of temperature (T), vapor residence time (t_v), and catalyst to oil ratio ($\varphi_{c/o}$) are observed. Typical results for FCC of feed no. 1 at different operation conditions are presented in Table 4. In this table, it can be known that the y_{GP}, y_{GO}, and y_{COKE} keep decreasing whereas y_{GN}, y_{DG}, y_{LCO}, and y_{GA} are always increasing when the temperature goes up; the y_{LPG} rises first and then decreases as temperature goes up; the y_{GP}, y_{GO}, and y_{GN} decrease whereas y_{GA}, y_{DG}, y_{LPG}, y_{LCO}, and y_{COKE} increase if vapor residence time or catalyst to oil ratio goes up whilst the other variables are same.

More than 50 sets of experimental data have been obtained in this work; among them, 30 sets of experimental data of feed nos. 1 and 2 are used to estimate kinetic constants of eight-lump kinetic model for secondary reaction of FCC gasoline according to hybrid genetic algorithm; 15 sets of experimental data of feed no. 3 are used to check the reliability of the model.

Since the key lumps of this reaction system are gasoline olefin lump and liquefied petroleum gas, the yields of both from feed nos. 1 and 2 at different temperatures, vapor residence times, and catalyst to oil ratios are presented in Figs. 3–6, respectively. These points in Figs. 3 and 4 are the experimental data of feed no. 1 and points in Figs. 5 and 6 are corresponding data of feed no. 2.

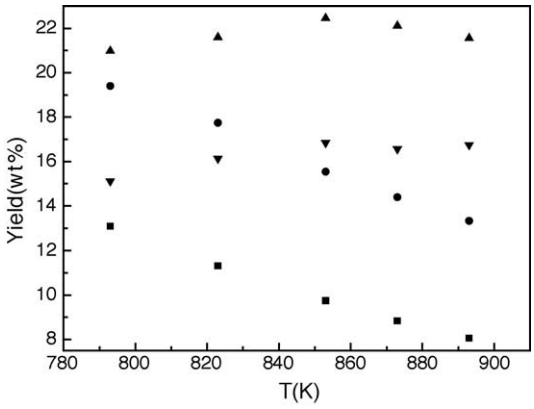

Fig. 3. GO (■ and ●) and LPG (▲ and ▼) yields of feed no. 1 vs. temperatures ($\varphi_{c/o} \approx 13.0$ (■ and ▲) and $\varphi_{c/o} \approx 8.0$ (● and ▼) with constant vapor residence time).

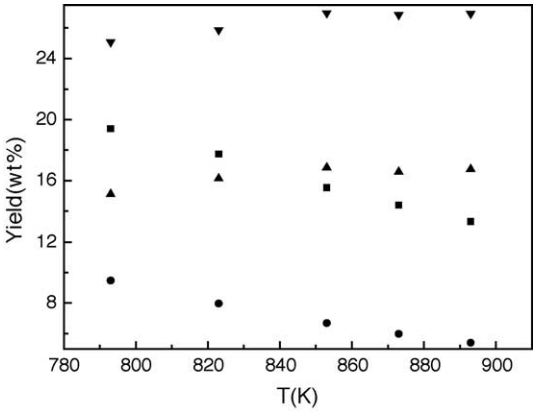

Fig. 4. GO (■ and ●) and LPG (▲ and ▼) yields of feed no. 1 vs. temperatures ($t_v \approx 2.0$ (■ and ▲) and $t_v \approx 4.0$ (● and ▼) with constant catalyst to oil ratio).

In Figs. 3 and 5, vapor residence time is kept constant and the effect of catalyst to oil ratio is researched. It can be known from these two figures that the yield of GO decreases whilst yield of LPG increases when the catalyst to oil ratio goes up. The yield of GO keeps decreasing gradually, the yield of LPG rises first and then goes down as operational temperature goes up. This fact indicates the over-cracking of liquefied petroleum gas lump components into dry gas under high temperature.

Table 4
Typical experimental results of secondary reactions for FCC of feed no. 1 at different conditions

T (K)	$\varphi_{c/o}$	t_v (s)	y_{GP} (%)	y_{GO} (%)	y_{GN} (%)	y_{GA} (%)	y_{DG} (%)	y_{LPG} (%)	y_{LCO} (%)	y_{COKE} (%)
823	8.0	2.0	28.70	17.74	9.85	19.11	1.48	16.14	4.54	2.13
823	8.0	4.0	24.57	7.97	6.55	21.27	2.64	25.87	5.18	5.27
823	13.0	2.0	26.30	11.32	8.12	20.82	2.21	21.59	5.05	3.78
853	8.0	2.0	27.86	15.54	10.43	20.02	2.56	16.85	4.39	2.02
853	8.0	4.0	23.58	6.69	6.52	21.79	4.12	26.98	5.13	4.93
853	13.0	2.0	25.40	9.74	8.27	21.51	3.47	22.45	4.95	3.58
873	8.0	2.0	27.33	14.39	10.71	20.43	3.40	16.57	4.31	1.95
873	8.0	4.0	22.91	5.99	6.51	21.97	5.42	26.87	5.09	4.67
873	13.0	2.0	24.78	8.84	8.35	21.82	4.58	22.11	4.89	3.41

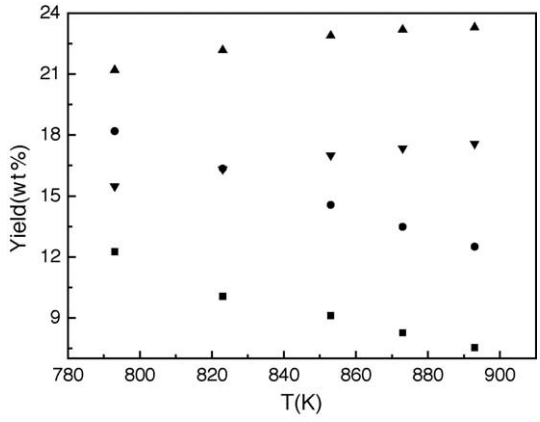

Fig. 5. GO (■ and ●) and LPG (▲ and ▼) yields of feed no. 2 vs. temperatures ($\varphi_{c/o} \approx 20.0$ (■ and ▲) and $\varphi_{c/o} \approx 13.0$ (● and ▼) with constant vapor residence time).

In Figs. 4 and 6, catalyst to oil ratio is kept constant and the effect of vapor residence time is researched. It can be known from these two figures that the yield of GO decreases whilst yield of LPG increases when the vapor residence time goes up. It also can be observed from these two figures that the yield of GO keeps decreasing whilst the yield of LPG rises first and then goes down as operational temperature goes up.

4.2. Calculation of rate constants

The eight-lump kinetic model for FCC gasoline secondary reactions contains 21 rate constants. It is very difficult to obtain so many parameters with a simple strategy. Traditionally, the whole reaction network needs to be logically transformed into several smaller subsidiary networks firstly; then, a series of experiments should be conducted for each subsidiary network. Improved non-linear regression procedures based on Marquardt's algorithm with the least squares criterion for the objective function were widely applied to find the best set of kinetic parameters [16]. For the eight-lump model of gasoline secondary reactions, the traditional methods confronted a problem of PONA components separation. It was too hard to get enough samples in the laboratory to perform experiments for the subsidiary networks.

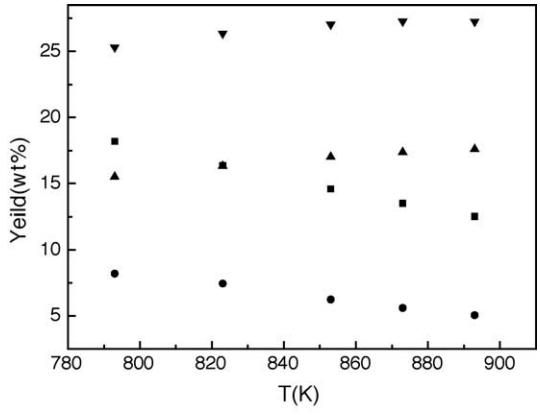

Fig. 6. GO (■ and ●) and LPG (▲ and ▼) yields of feed no. 2 vs. temperatures ($t_v \approx 2.0$ (■ and ▲) and $t_v \approx 3.0$ (● and ▼) with constant catalyst to oil ratio).

A hybrid optimization method that includes genetic algorithm, evolution strategy, and annealing algorithm developed by authors [17] was used in this work. The genetic algorithm is widely used to solve the optimization problems in the field of chemical engineering including kinetic parameter estimation [18–21]. A notable characteristic of this algorithm is that it can find the region of the optimal values quickly; however, the ability of accurate search in this region is not satisfactory for complex system. In the new hybrid method, the normal genetic algorithm was modified with adaptive multi-annealing crossover and mutation strategies instead of simple strategy. The multi-pattern evolution was also adapted to improve the search efficiency. This hybrid algorithm can avoid the problem of local optimum and show a higher estimating precision, a better convergence than that the normal genetic algorithm.

(1) For the system of secondary reactions in catalytically cracked gasoline, the criterion function is defined as:

$$\text{fitness}\,(\tilde{K}) = \left[\sum_{j=1}^{m}\left(\frac{|y_j^{\mathrm{c}} - y_j^{\mathrm{e}}|}{y_j^{\mathrm{e}}}\right)\right]^{-1} \tag{14}$$

where m is the lumps numbers, y_j^{c} is the calculated yield of jth lump in an individual of certain generation in evolutionary process of the algorithm and is the function of the parameters $\tilde{K}$ and y_j^{e} is the corresponding experimental one. It corresponds to the adaptation of each individual to transfer itself to the new generations. The higher the value of fitness is, the more chance likely the individual will be kept during the selection step.

(2) The real number coding was preferred. It is better than binary coding because that the genes of each individual can get any necessary precision.

(3) A $(\mu + \lambda)$ evolution strategy was employed as selection strategy. In this strategy, a population consists of μ parents, each of which is uniquely characterized by a certain number of parameters. Per generation, a certain number λ of children are created by selecting chromosomes at random from the parent population's gene pool. The chromosomes of children are created by the operation of recombination and random mutation. From the total population of $\mu + \lambda$ individuals, the μ fittest ones are selected to consist the next generation. This is a multi-point searching method; it uses truncation selection in an extended searching space and can retain the excellent individuals of parent and child generation.

(4) The adaptive multi-annealing mutation, adaptive multi-annealing crossover and population strategy are introduced into the genetic algorithm to improve the performance and to reduce the cost of CPU time.

Since one set of experimental data includes the product yields of eight lumps and the information about temperature,

Table 5
Results of reaction kinetic parameters estimated by hybrid evolution-simulated annealing algorithm with multi-pattern evolution

$k = f(T)\,(m^3\,(g_{cat}\,s)^{-1})$	E_{ji}
$k_{GP,GP} = \exp(2.4664 - 2830/T)$	23036 ± 45
$k_{GP,DG} = \exp(4.3282 - 4329/T)$	35991 ± 27
$k_{GP,LPG} = \exp(1.6540 - 1888/T)$	15697 ± 16
$k_{GP,COKE} = \exp(4.3775 - 4920/T)$	40905 ± 30
$k_{GO,GP} = \exp(2.0565 - 1775/T)$	14757 ± 43
$k_{GO,GN} = \exp(1.3698 - 1096/T)$	9112 ± 13
$k_{GO,DG} = \exp(3.2172 - 3169/T)$	26347 ± 22
$k_{GO,LPG} = \exp(2.3665 - 1574/T)$	13086 ± 80
$k_{GO,LCO} = \exp(0.7626 - 1221/T)$	10151 ± 29
$k_{GO,COKE} = \exp(5.1227 - 4975/T)$	41362 ± 36
$k_{GN,GO} = \exp(0.6411 - 867/T)$	7208 ± 42
$k_{GN,GA} = \exp(1.8989 - 1894/T)$	15747 ± 29
$k_{GN,DG} = \exp(4.7073 - 5235/T)$	43524 ± 73
$k_{GN,LPG} = \exp(1.4000 - 1795/T)$	14924 ± 56
$k_{GN,LCO} = \exp(6.4059 - 6720/T)$	55870 ± 22
$k_{GN,COKE} = \exp(3.8854 - 3801/T)$	31602 ± 49
$k_{GA,DG} = \exp(-1.7427 - 1865/T)$	15506 ± 24
$k_{GA,LCO} = \exp(1.8889 - 3786/T)$	31477 ± 17
$k_{GA,COKE} = \exp(0.3454 - 1607/T)$	13361 ± 58
$k_{LPG,DG} = \exp(-0.0837 - 1974/T)$	16412 ± 71
$k_{LCO,COKE} = \exp(1.7184 - 3126/T)$	25990 ± 72

catalyst to oil ratios and vapor residence times in this case, it can be used to get an optimal unique solution including 21 kinetic parameters by the hybrid optimization method developed by authors, therefore, 30 sets of experimental data from feed nos. 1 and 2 with the temperature range from 793 to 873 K can get 30 sets of these kinetic constants. The final parameters ($\bar{K}$) of the kinetics model can be obtained by taking the average value in each temperature. According to the Arrhenius equation, the activation energy E_{ji} thus can be calculated by linear regress with the $\bar{K}$ data in different temperatures.

The value of objective function fitness can be obtained by numerical integration of Eq. (12) using Runge-Kutta method in each generation, all the values of the objective function gained in the end of each calculation are greater than 500, it means the average relative error for each lump between calculation and experiment is less than 0.00025.

Table 5 shows the estimated values of average activation energies and the expressions of the kinetics constants. The 95% probability intervals show the E_As estimated are quite precisely as shown in this table.

4.3. Verification of the model

The kinetic model, together with the parameters shown in Table 5, was used to predict the results of secondary reactions of FCC naphtha feed no. 3. The comparison of the key lumps between predicted result (solid lines) and experimental data (marks) is shown in Figs. 7 and 8, respectively.

From these two figures, it can be known that the experimental results fit the predicted product yields very well, which indicates that the model of eight lumps is reliable and the kinetic constants estimated according to hybrid genetic algorithm are reasonable.

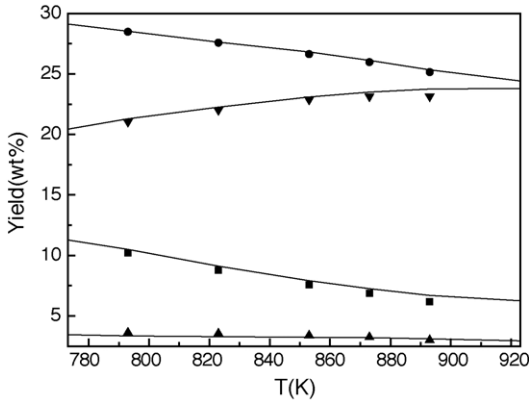

Fig. 7. Predicted and experimental product yields of feed no. 3 for GP (●), GO (■), LPG (▼), and COKE (▲) (catalyst to oil ratio of 2.0 and vapor residence time of 13.0 s).

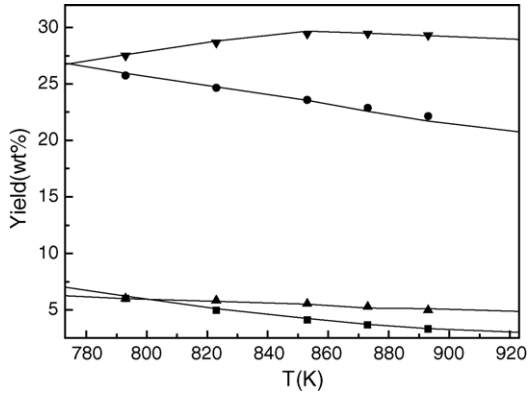

Fig. 8. Predicted and experimental product yields of feed no. 3 for GP (●), GO (■), LPG (▼), and COKE (▲) (catalyst to oil ratio of 3.0 and vapor residence time of 12.0 s).

Table 6 is the comparison of the yields for all the lumps between predicted and experimental results from feed no. 3 at different temperature, catalyst to oil ratio and vapor residence time. The comparison result shows that the model performs well in the extended operation area.

Table 6
Comparison of the product yields between predicted and experimental results from feed no. 3

Items	Run 1		Run 2	
	Experimental	Predicted	Experimental	Predicted
T (K)	773		923	
t_v (s)	2.0		1.7	
$\varphi_{c/o}$	9.5		9.0	
y_{GP} (%)	28.96	28.10	25.85	25.21
y_{GO} (%)	10.27	9.97	12.00	11.81
y_{GN} (%)	13.50	14.20	11.26	11.99
y_{GA} (%)	22.49	22.75	20.94	21.22
y_{DG} (%)	3.90	3.20	6.43	6.77
y_{LPG} (%)	13.96	14.33	17.22	16.89
y_{LCO} (%)	4.65	4.79	4.20	4.58
y_{COKE} (%)	2.27	2.57	1.68	1.94

5. Conclusions

In accordance with the PONA components of cracked gasoline and the characteristics of product structures, the reaction scheme has been established following the analysis and discussion on the reaction mechanism, eight-lump kinetic model for secondary reactions of FCC gasoline has been set up.

Twenty-one kinetic constants and corresponding activation energy values were gained according to the evolutionary-simulated annealing algorithm with multi-pattern evolution. This algorithm can avoid local optimum effectively and made it possible to get the model parameters precisely.

The calculated data of the kinetic model were verified with experimental results. It shows that predicted product distribution agrees well with the experimental results, the kinetic parameters calculated from the algorithm are reliable, and the model is better in its extrapolability.

Acknowledgements

Financial support for this work from the Key Project of National Natural Science Foundation of China (20436040), National Natural Science Foundation of China (20476084) and China Petroleum & Chemical Corporation (03103057) are gratefully acknowledged.

References

[1] T.M. John, B.M. Wojciechowski, On identifying the primary and secondary products of the catalytic cracking of neutral distillates, J. Catal. 37 (1975) 240–249.
[2] V.W. Weekman, A model of catalytic cracking conversion in fixed, moving, and fluid-bed reactors, Ind. Eng. Chem. Proc. Des. Dev. 7 (1968) 90–95.
[3] V.W. Weekman, D.M. Nace, Kinetic of catalytic cracking selectivity in fixed, moving and fluid bed reactors, AIChE J. 16 (1970) 397–401.
[4] J. Corella, E. Frances, Analysis of the riser reactor of a fluid catalytic cracking unit, in: M.L. Occelli (Ed.), Fluid Catalytic Cracking II: Concept in Catalyst, American Chemical Society, Washington, DC, 1991, pp. 165–167 (Chapter 10).
[5] J. Ancheyta-Juarez, F. Lopez-Isunza, E. Aguilar-Rodriguez, Five-lump kinetic model for gas oil catalytic cracking, Appl. Catal. A Gen. 177 (1999) 227–235.
[6] M.M. Sungungun, I.M. Kolesnikov, V.M. Vinogradov, S.I. Kolesnikov, Kinetic modeling of FCC process, Catal. Today 43 (1998) 315–325.
[7] B. Gross, S.M. Jacob, D.M. Nace S.E. Voltz, Simulation of catalytic cracking process, US Patent 3,960,707 (1976).
[8] X.L. Deng, Y.X. Sha, L.Y. Wang, G.L. Wang, F.D. Meng, Study on a kinetic model of resid catalytic cracking, Pet. Process. Petrochem. 8 (1994) 35–39.
[9] W.M. Raymond, R. Terry, X.J. Zhao, Suppressing FCC gasoline olefinicity while managing light olefins production, in: NPRA Annual Meeting, AM-98-11, San Francisco, 1998.
[10] X. Ye, W. Jiao, Y. Liu, et al., Chinese refinery uses new catalyst to meet olefin regulation, Oil Gas J. 30 (2000) 66–69.
[11] Y. Xu, J. Zhang, J. Long, et al., A modified FCC process for maximizing isoparaffins in cracked naphtha, Acta Petrolei Sinica (Pet. Process. Sect.) 1 (2003) 43–47.
[12] L.Y. Wang, B.L. Yang, G.L. Wang, Z.B. Li, J.L. Wei, New FCC process minimizes gasoline olefin, increase propylene, Oil Gas J. 6 (2003) 52–58.
[13] J. Wei, C.W. Kuo, A lumping analysis in monomolecular reaction systems, Ind. Eng. Chem. Fundam. 1 (1969) 114–123.
[14] C.W. Kuo, A. Wei, A lumping analysis in monomolecular reaction systems, Ind. Eng. Chem. Fundam. 1 (1969) 124–133.
[15] J. Chen, H. Cao, Catalytic Cracking Technology and Engineering, China Petrochemical Press, Beijing, 1995, pp. 138–144.
[16] S.D. Harris, L. Elliott, D.B. Ingham, M. Pourkashanian, C.W. Wilson, The optimization of reaction rate parameters for chemical kinetic modeling of combustion using genetic algorithms, Comput. Method Appl. M. 8–10 (2000) 1065–1090.
[17] F.X. Meng, B.L. Yang, R.Q. Yao, X.H. Tao, Kinetic study on synthesis reaction of methyl *tert*-butyl ether by using hybrid evolutionary algorithm, J. Chem. Ind. Eng. (China) 3 (2003) 327–332.
[18] S.B. Yang, B.L. Yang, Estimating kinetics parameters in synthesis of ethyl *tert*-butyl ether by using genetic algorithm, J. Chem. Ind. Eng. (China) 53 (2002) 54–59.
[20] R.Q. Yao, B.L. Yang, Kinetics research for the synthesis of branch ether using genetic-simulated annealing algorithm with multi-pattern evolution, Chem. Eng. J. 2 (2003) 113–119.
[21] M. Maeder, Y.M. Neuhold, G. Puxty, Application of a genetic algorithm: near optimal estimation of the rate and equilibrium constants of complex reaction mechanisms, Chemometr. Intell. Lab. 70 (2004) 193–203.